Charting the dynamic methylome across the human lifespan

Slieker, R.

Age-related DNA methylation changes are tissue-specific but share functional elements

Roderick C. Slieker[1], Caroline L. Relton[2], Tom Gaunt[2], P. Eline Slagboom[1], Bastiaan T. Heijmans[1]

[1] *Molecular Epidemiology section, Leiden University Medical Center, The Netherlands*
[2] *School of Social and Community Medicine, University of Bristol, Bristol, United Kingdom*

ABSTRACT

While associations between DNA methylation and chronological age are well-established and chronological age can be accurately predicted from DNA methylation, most studies focused on blood and little is known on tissue-shared and tissue-specific age-related DNA methylation changes.

To investigate the tissue-dependency of age-related changes we identified and characterized age-related differentially methylated position (aDMPs) in public data of seven tissues including brain (N=603), buccal (N=96), liver (N=147), kidney (N=171), subcutaneous fat (SAT, N=648), monocytes (N=1,202) and T-helper cells (Th cells, N=214) using the Illumina 450k array. aDMPs were defined as CpGs with a significant ($P_{bonf} \leq 0.05$) gain or loss of methylation of ≥2% per 10 years. Out of the 428,279 CpGs investigated, 7,850 aDMPs gained DNA methylation in one or more tissues (gain-aDMPs) and 4,287 aDMPs lost DNA methylation in one or more tissues (loss-aDMPs). The majority of the aDMPs were tissue-specific (gain-aDMPs:85.2%; loss-aDMPs: 97.4%), although the overlap between gain-aDMPs was relatively higher compared to loss-aDMPs. Gain-aDMPs occurred almost exclusively at CpG islands (42%-88%) and affected CpG islands were also tissue-specific (70.1%) and so were the genes near gain-aDMPs (64.8%). Loss-aDMPs often resided in regions marked by active histone modifications and also genes near loss-aDMPs were tissue-specific (83.6%). Genes near gain-aDMPs related to developmental processes, while genes near loss-aDMPs were involved in cell motion and signal transduction.

Together, these results show that age-related gain and loss of DNA methylation in multiple tissues target the same type of functional elements, but at the CpG, functional element and gene level they are tissue-specific, implicating that the loss of epigenetic control with age is tissue-specific.

Supplementary figures can be found in Appendix IV

INTRODUCTION

The association between DNA methylation and chronological age is well-established in whole blood (Bell et al., 2012; Dozmorov, 2015; Florath et al., 2014; Garagnani et al., 2012; Johansson et al., 2013; Marttila et al., 2015; McClay et al., 2014; Rakyan et al., 2010; Steegenga et al., 2014; Yuan et al., 2015). However, also in adipose tissue, brain and hMSCs, loci have been found where DNA methylation closely track the chronological age (Fernández et al., 2014; Hernandez et al., 2011; Rönn et al., 2015). The association between DNA methylation and chronological age has been shown to be a powerful tool to predict chronological age. Multiple predictors have been developed that can estimate the chronological age based on the DNA methylation status of sets of CpG sites. Two predictors are specific for blood, while the age predictor by Horvath is independent of the tissue studied (Hannum et al., 2013; Horvath, 2013; Weidner et al., 2014). The tissue-independency of the Horvath age predictor suggests that in every tissue different CpGs contribute to the prediction of chronological age or that there are CpGs that are tissue-independent (Bekaert et al., 2015). Evidence for the latter exists as in two studies using the 27k array, in which it was shown that >60% of the aDMPs in whole blood are concordant in effect size direction in other tissues (Xu and Taylor, 2014) and that aDMPs found in tissues show overlap among each other (Day et al., 2013). Moreover, the CpGs near the *ELOVL2* gene are examples of tissue-independent age-related changes as they have been identified in multiple tissues, including blood, hMSCs (Fernández et al., 2014) and teeth (Bekaert et al., 2015). Even in mice CpGs near *ELOVL2* track chronological age (Spiers et al., 2016).

These studies suggest that the epigenetic loss of control is tissue-independent. Yet, the functional changes that are observed in tissues are far from tissue-independent, where each tissue has its own tissue-specific functional age-related change (Richardson et al., 2014). This makes tissue-independent epigenetic changes counterintuitive, as one would expect a tissue-specific epigenetic changes. To further explore the tissue-specificity of aDMPs, we identified and characterized age-related DNA methylation changes in 7 tissues using the 450k array.

RESULTS

To investigate age-related DNA methylation changes between tissues, Illumina 450k DNA methylation data of 16 tissues were obtained from public repositories, encompassing in total 8,092 samples (**Table S1**). First, we investigated the age-related differentially methylated position (aDMP) near *ELOVL2* (cg16867657), to investigate whether the tissue-independent character of this aDMP extended to more tissues than described in literature. Gain of methylation was observed in blood (N=4674, **Figure 1A**) and extended to most of the 16 tissues investigated (**Figure 1B**). However, the slope at which tissues gained DNA methylation was different between tissues, where buccal showed the highest age-related gain of methylation (**Figure 1B**). Within the brain, differences were observed between brain regions in the rate of gain of DNA methylation, where the dorsolateral prefrontal cortex (DLPFC) showed the strongest gain of DNA methylation with age, in contrast to the cerebellum, which almost did not gain DNA methylation over time.

The tissue-specific rate of age-related gain of methylation of the *ELOVL2* CpG,

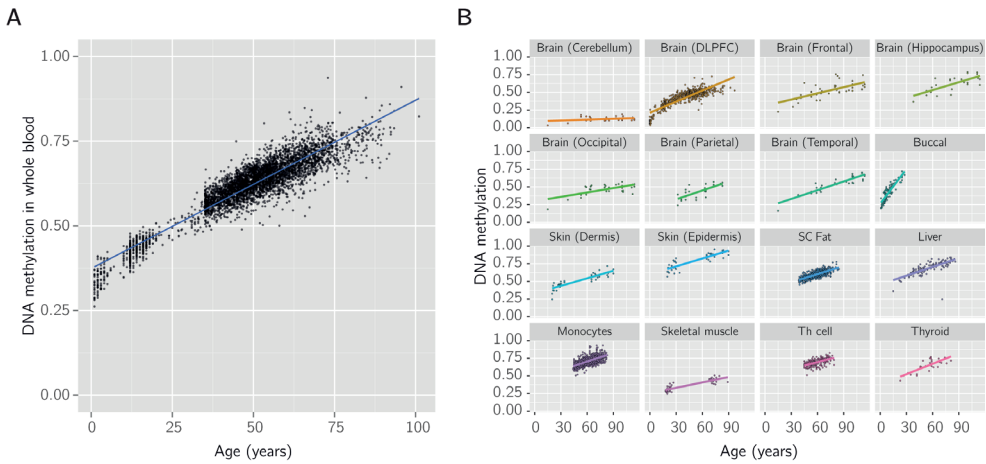

Figure 1 Age-related change in DNA methylation in ELOVL2. A DNA methylation (y-axis) against age (x-axis) in blood for the ELOVL2 CpG (cg16867657). B DNA methylation (y-axis) against age (x-axis) in other tissues for the ELOVL2 CpG (cg16867657).

raises the question to what extent age-related changes are tissue-specific. To this end, we identified aDMPs in tissues with a large sample size (96≤N≤1,202, **Table S1**), which included brain (N=603), buccal (N=96), liver (N=147), kidney (N=171), subcutaneous fat (SAT, N=648), monocytes (N=1,202) and T-helper cells (Th cells, N=214). We included aDMPs in subsequent analyses if the association with age was genome-wide significant ($P_{bonf} \leq 0.05$) and if the age-related gain or loss was greater than 2% per 10 years. Out of the 428,279 CpGs investigated, 7,850 aDMPs gained DNA methylation in one or more tissues (gain-aDMPs) and 4,287 aDMPs lost DNA methylation in one or more tissues (loss-aDMPs). The number of aDMPs identified in each tissue varied strongly, with the highest number in buccal (4857 aDMPs in N=96; **Figure 2A**) and the lowest number in Th cells (39 aDMPs in N=214). The number of gain- versus loss-DMPs differed between tissues, for example in liver aDMPs mainly gained DNA methylation (gain:2499, loss:411, **Figure 2A**), while in monocytes aDMPs mainly lost DNA methylation (gain:83, loss:574). The differences in number per tissue were driven neither by the known replication rate of the stem cells (r=0.14, *P*=0.79, **Figure S1A**) (Tomasetti and Vogelstein, 2015), nor by the number of samples used in each tissue (r=-0.28, *P*=0.54, **Figure S1B**). The differences in magnitude of gain and loss with age as observed for *ELOVL2*, were also found in the other identified aDMPs, where particularly buccal showed a strong age-related gain or loss of DNA methylation (**Figure 2B**).

The majority of aDMPs are tissue-specific

To access the tissue-dependency of aDMPs, we calculated per tissue the overlap of gain- or loss-aDMPs with aDMPs in other tissues. The large majority of aDMPs were tissue-specific, although the overlap was higher for gain-aDMPs compared to loss-aDMPs (**Figure 2C**). Of the gain-aDMPs, 1161 (14.8%) were identified in ≥2 tissues (**Figure 3A**). Only 2 gain-aDMPs were found in all 7 tissues studied and both mapped to the *ELOVL2* locus (**Table S3**).

The low overlap between tissue raises the question what fraction of the Horvath clock

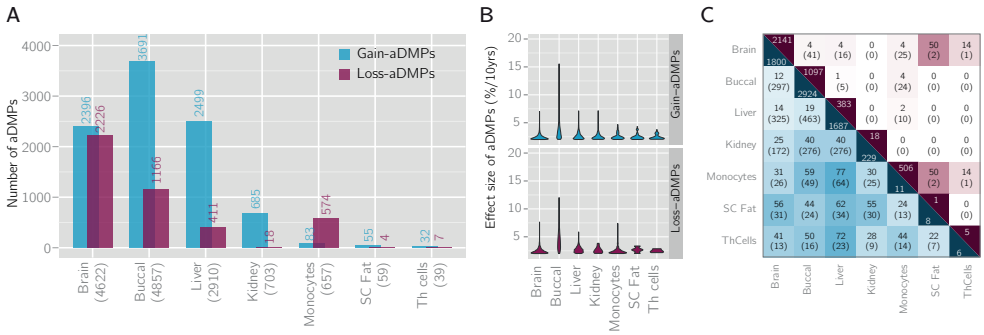

Figure 2 Identification of aDMPs. A Number of identified gain- and loss-aDMPs (y-axis) in this study for each tissue (x-axis). B Slopes of identified gain- and loss-aDMPs (y-axis) for each tissue (x-axis). C Overlap between tissues in identified gain- and loss-aDMPs. In the diagonal cells the number of aDMPs unique for that tissue, the upper number represents the percentage, the lower number the number of overlapping aDMPs. Blue – gain-aDMPs; Purple – loss-aDMPs

overlaps with the identified aDMPs in various tissues. Yet, the overlap the Horvath CpGs and here identified aDMPs was low (**Figure S2**). The highest overlap with gain-aDMPs was found in the brain (13 gain-aDMPs) and with loss-aDMPs in monocytes (N=6 loss-aDMPs). This illustrates Horvath's CpGs are different CpG sites than those that show a large age-related change in various tissues.

In the primary dataset we used different sets of individuals in each tissue. To exclude that the differences between tissues were driven by the fact that they originate from different individuals, we determined the slope of aDMPs in a dataset comprising 10 tissues (blood, subcutaneous fat, heart, kidney, kidney fat, liver, muscle, omentum, skin and spleen) of the same individual (10-16 individuals per tissue, age range 44-85 years, **Table S1**). Unique and overlapping aDMPs in liver, kidney, SAT, monocytes and Th cells were also observed in this independent dataset (**Figure S3**). Observed age-related changes were, however, often specific for that tissue only. For example, the slopes of liver gain-aDMPs were high in the liver, kidney and to some extent spleen, but not in the other tissues (**Figure S3**). Likewise, liver loss-aDMPs were low in the liver and spleen in contrast to other tissues. These results suggest that age-related changes in one tissue are not indicative of age-related changes in another tissue.

Gain-aDMPs are tissue-specific but share functional elements

To explore the overrepresentation of gain-aDMPs in specific functional elements in primary tissues, we compared aDMPs to previously published chromatin state segmentations which mark genomic function based on combinations of histone modifications (Roadmap Epigenomics Consortium et al., 2015). Gain-aDMPs were overrepresented at segmentations marked by the histone modification H3K27me3, including Bivalent Enhancers (OR:2.8-8.0, $P<0.0001$, **Figure 3B**) and Repressed Polycomb (3.4-9.8, $P<0.0001$). Next, we compared gain-aDMPs to a CGI-centric annotation (CpG island, shore (+-2kb) and non-CGI). The majority of age-related gain of methylation occurred at CpG islands and their shores (OR=1.6-15.6, $P<0.0001$, **Figure 3C**). Comparison of gain of methylation with ENCODE transcription factor

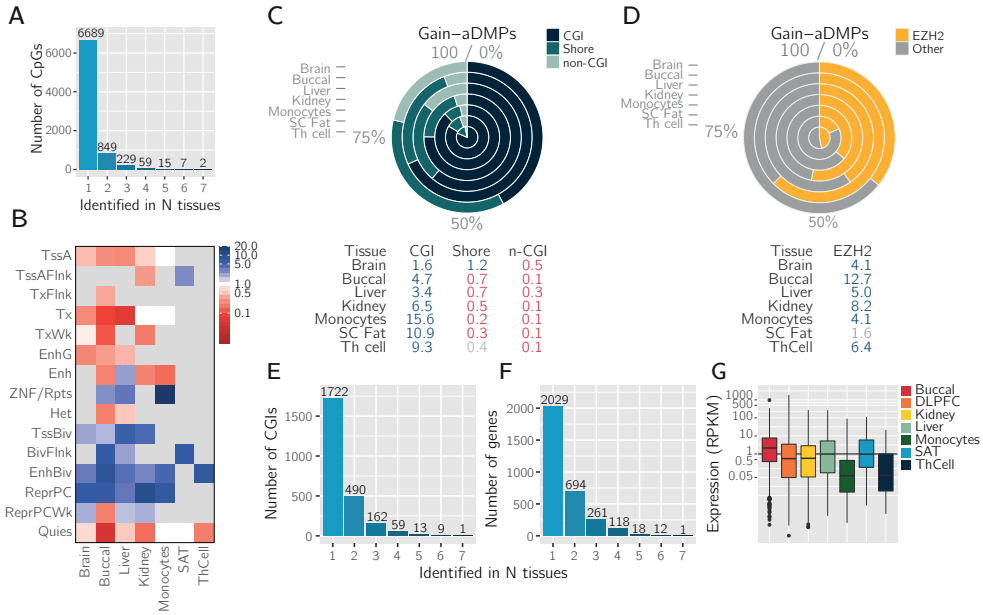

Figure 3 Characterization of gain-aDMPs. A Frequency of aDMPs (y-axis) against the number of tissues the aDMPs was identified in (x-axis). B Enrichment of gain-aDMPs in chromatin segmentations expressed as an odds ratio, grey non-significant. C Percentage (top) and odds ratios (bottom) of aDMPs in CGIs, shores and non-CGIs. Blue enriched, red depleted, grey non-significant. D Percentage (top) and odds ratios (bottom) of aDMPs in EZH2 binding sites (ChIP-seq, any cell type, ENCODE). Blue enriched, red depleted, grey non-significant. E Frequency of CpG islands (y-axis) against the number of tissues a CpG island was identified in (x-axis). F Frequency of genes (y-axis) against the number of tissues a gene was identified in (x-axis). G Expression (y-axis, RPKM) of genes near gain-aDMPs per tissue (x-axis). Abbreviations: TssA, Active TSS; TssAFlnk, Flanking active TSS; TxFlnk, Transcr. at gene 5' and 3'; Tx, Strong transcription; TxWk, Weak transcription; EnhG, Genic enhancers; Enh, Enhancers; ZNF/Rpts, ZNF genes+repeats; Het, Heterochromatin; TssBiv, Bivalent/Poised TSS; BivFlnk, Flanking bivalent TSS/Enh; EnhBiv, Bivalent enhancer; ReprPC, Repressed Polycomb; ReprPCWk, Weak repressed Polycomb, Quies, Quiescent/low

binding sites showed that many of the gain-aDMPs overlapped with binding sites of Polycomb (PcG) repressive complex 2 (PRC2) protein EZH2 (any cell type, ChIP-seq, ENCODE), in line with the enrichment for Repressed Polycomb. In each of the tissues, about a third of the identified gain-aDMPs overlapped with an EZH2 binding site up to even over 60% in buccal (OR=12.7, $P<0.0001$, **Figure 3D**). To address what characteristic was underlying to the gain of DNA methylation (CGI, EZH2 or both) we directly compared aDMPs that overlapped with CGIs and EZH2. EZH2-CGIs were 2-fold enriched (1.9-2.8, $P<0.0001$) compared to aDMPs that overlapped with CGI or EZH2 only (**Figure S4A**). This suggesting that the EZH2 bound CGI is more likely to gain DNA methylation than regions with one of these characteristics.

CGIs and genes that gain methylation are also tissue-specific

To explore whether not only CpGs were tissue-specific, but also the genomic feature and the gene they target, we investigated the overlap of affected CGIs and genes in each tissue. Similar to the gain-aDMPs were the CpG islands that gain DNA methylation tissue-specific (1722 CGIs, 70.1%, **Figure 3E**). Furthermore, genes near gain of DNA methylation were tissue-specific, where 2029 genes were unique for a tissue (64.8%). The one gene that was identified in all 7 tissues was again the *ELOVL2* gene (**Figure 3F** and **Table S3**). Among the 12 genes that were identified in 6 tissues, genes of interest were observed including *BMI1* and *LIN28B*. *BMI1* is involved in DNA damage and part of the PRC1 complex (Ismail et al., 2012). *LIN28B* is a microRNA that enhances IGF-2 translation (Polesskaya et al., 2007). The tissue-specificity of genes was further confirmed, when in each tissue for each gene the frequency of nearby gain-aDMPs was calculated. In each tissue, genes were identified where the frequency of gain-aDMPs was high in one tissue (>5 CpGs), but low in other tissues (**Table S4**), such as *PRRT1* in the brain (brain: 24, buccal:5, liver:7, kidney:1, monocytes:0, SAT:1, Th cell:2) and *HOXD* in buccal (buccal:26, other tissues:0). So, the majority of genes gain DNA methylation in one tissue and if genes overlap between tissues, the number of gain-aDMPs near the overlapping gene is often high in one tissue, but low in the others.

Next, we investigated the function of genes near gain-aDMPs, by comparing them to gene ontology (GO) gene sets per tissue. In brain (84 processes), buccal (151 processes), liver (64 processes) and kidney (59 processes) significant enrichments (P_{bonf}≤0.05) were found for genes near gain-aDMPs. Processes that were common among the top enriched GO terms were embryonic morphogenesis (Number of genes in brain: 82, buccal: 98, liver: 69, kidney: 37; P_{bonf}<0.0001, **Table S5**) and regulation of transcription (Number of genes in brain: 231, buccal: 318, liver: 209, kidney: 134; P_{bonf}<0.0001, **Table S5**). Finally, we investigated the gene expression of genes near gain-aDMPs, by using public gene expression data of matching tissues (GTEX data, frontal cortex, N=108; esophagus – mucosa, N=286; liver, N=119; kidney cortex, N=32; whole blood, N=393; age-range 20-79 years). In line with the developmental character of genes near gain-aDMPs, the expression was low and the expression remained constant over with age (**Figure 3G** and **Figure S4B**). That these genes do not change in expression with age, was further confirmed as we found a low overlap between genes near gain-aDMPs and genes with age-related differential (brain: 91, buccal: 104, liver: 88, kidney:28, monocyte:1, SAT:3, Th cell: 0) (Peters et al., 2015).

Loss-aDMPs are enriched for active regions including tissue-specific enhancers

In contrast to gain-aDMPs, loss-aDMPs were often found in non-CGI regions (OR: 1.3-9.1, *P*<0.0001, **Figure 4A**). Loss-aDMPs were more tissue-specific than gain-aDMPs, as 4176 loss-aDMPs (97.4%) were unique for one tissue and only 111 loss-aDMPs (2.6%) were found in ≥2 tissues (**Figure 4B**). We further explored the functionality of loss-aDMPs per tissue by comparing them to previously published chromatin state segmentations of matching primary tissues. Loss-aDMPs were particularly overrepresented at chromatin states marking an active genome (**Figure 4C**). In 5 tissues enrichment was found for Enhancers: in the brain (OR:6.6, *P*<0.0001, **Figure 4C**), buccal (OR:2.7, *P*<0.0001), liver (OR:1.6, *P*<0.001), monocytes (OR:2.9,

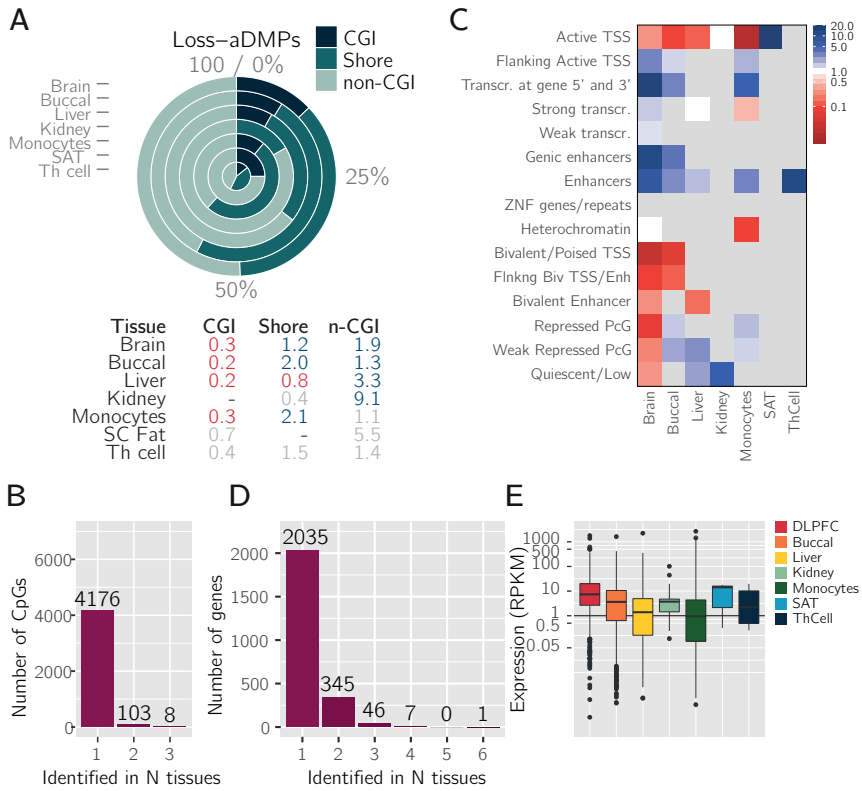

Figure 4 Characterization of loss-aDMPs. A Percentage and odds ratios of aDMPs in CGIs, shores and non-CGIs. Blue enriched, red depleted, grey non-significant. B Number of tissues an aDMPs was identified in. C Enrichment of gain-aDMPs in chromatin segmentations expressed as an odds ratio, gray non-significant enrichment. D Frequency of genes (y-axis) against the number of tissues an genes an aDMP was identified in (x-axis). E Expression of genes (y-axis, RPKM) near loss-aDMPs per tissue (x-axis). Abbreviations: TssA, Active TSS; TssAFlnk, Flanking active TSS; TxFlnk, Transcr. at gene 5′ and 3′; Tx, Strong transcription; TxWk, Weak transcription; EnhG, Genic enhancers; Enh, Enhancers; ZNF/Rpts, ZNF genes+repeats; Het, Heterochromatin; TssBiv, Bivalent/Poised TSS; BivFlnk, Flanking bivalent TSS/Enh; EnhBiv, Bivalent enhancer; ReprPC, Repressed Polycomb; ReprPCWk, Weak repressed Polycomb, Quies, Quiescent/low

P<0.0001) and Th cells (OR:11.2, *P*<0.001) and Genic enhancers in 2 tissues (brain, OR:11.9, *P*<0.0001; buccal, OR:3.6, *P*<0.0001). Moreover, loss-aDMPs were overrepresented at active transcribed regions, including Transcribed at 3'and 5' in brain (OR:14.5, *P*<0.0001), buccal (OR:3.0, *P*<0.0001) and monocytes (OR:4.6, *P*<0.01). Next, we mapped loss-aDMPs to their nearest gene and compared the overlap between genes. The majority of genes was unique (2035 genes, 83.6%, **Figure 4D**). Loss-aDMPs were found near *CD46* in 6 tissues and in 4 tissues loss-aDMPs were found near *KCNQ1*, *FAM92B*, *PLEC*, *GSE1*, *BAIAP2*, *PRDM16*, *ACTG1* (**Table S6**). The genes that were identified in multiple tissues have a 'housekeeping' function, for example *PLEC*, *BAIAP2*, *ACTG1* play a role in the maintenance of the cytoskeleton. Next we

investigated the frequency of loss-aDMPs near genes. As observed for the gain-aDMPs, a large number of loss-aDMPs were exclusively observed in one tissue. For example, 24 loss-aDMPs were identified near *DIP2C* in the brain, against low numbers in other tissues (buccal:1, liver:3, kidney:0, monocytes:0, SAT:0, Th cell:0). In buccal, 18 CpGs lost DNA methylation near *SLC7A5*, while no loss-aDMPs were found near this gene in other tissues (**Table S7**). To investigate the role of all identified genes in a tissue, we compared the genes with GO gene sets. Only brain showed a significant overlap with gene sets that related to signal transduction and motility, including regulation of Small GTPase mediated signal transduction (43 genes, P_{bonf}<0.0001) and Regulation of cell motion (33 genes, P_{bonf}<0.05, **Table S8**). However, among the top 10 of the other tissues, also GO terms related to intracellular signaling and cell motility were found to be overrepresented (P<0.05). Finally, we investigated the expression of genes near loss of DNA methylation and the expression of these genes was moderate (**Figure 4E**). Furthermore, the expression remained constant over time (**Figure S4C**) and similar to genes near gain-aDMPs, a low overlap was found with previously identified age-related differentially genes in blood (brain: 114; buccal:77, liver:23, kidney:3, monocyte:36, SAT:0, Th cell:1).

DISCUSSION

Here, we identified and characterized aDMPs in published datasets covering 7 tissues of different populations. The majority of the aDMPs were tissue-specific. Of the tissue-independent aDMPs, most aDMPs gained DNA methylation with age. Of the latter, the *ELOVL2* promoter is an example of a locus that is exceptionally consistent across tissues. Gain of DNA methylation almost exclusively occurred at CpG islands and their flanking shores and often overlapped with regions to which the repressive protein EZH2 binds. The majority of CpG islands and nearest genes that gained methylation over time were also tissue-specific, illustrating that gain of methylation occurs at different CGIs and genes and not just different CpGs. Loss-aDMPs were enriched for active regions, including enhancers. Genes near gain-aDMPs were associated with developmental processes and lowly expressed, while genes near loss-aDMPs were associated with signal transduction and cell motility.

The tissue-specific character of aDMPs raises the question what mechanism underlies the age-related changes – especially since there is resemblance in the type of genomic elements that show age-related gain of DNA methylation. Age-related changes at regions marked by polycomb have been found in several studies investigating blood (Dozmorov, 2015; Rakyan et al., 2010; Teschendorff et al., 2010; Yuan et al., 2015) and have been found in other species (Maegawa et al., 2010; Spiers et al., 2016). A proposed theory for the gain of DNA methylation on CpG islands may be loss of binding – or erosion – of the polycomb repressive complex 2 protein from the DNA (PRC2) (Jung and Pfeifer, 2015). Promoters overlapping with a CGI of genes that are lowly expressed, are kept in a repressive state. Some of these promoters are kept repressed by the repressive complex PRC2 and EHZ2 is part of this complex. Age-related loss of repression would allow DNA methyltransferases (DNMTs) to de novo methylate CGIs (Jung and Pfeifer, 2015). However, if true, it would require that some regions are more susceptible to age-related erosion of PRC2 and this should concern different regions in each tissue.

In contrast to gain-aDMPs, loss-aDMPs were found to overlap with active regions,

such as enhancers. This is in line with studies in blood and hMSCs that show that age-related loss preferentially occurs at enhancers (Dozmorov, 2015; Fernández et al., 2014; Peters et al., 2015). Genes near loss-aDMPs were not associated with tissue-specific processes, but instead with generic processes such as intracellular signaling cascade and cell motility pathways. Loss-aDMPs in blood has been identified before with similar processes (Steegenga et al., 2014).
Although the mechanisms driving age-related DNA methylation changes remain inconclusive, the functional consequences it has are also limited. Previous studies showed that DNA methylation of aDMPs is only limited associated with expression of nearby genes (Reynolds et al., 2014; Steegenga et al., 2014; Yuan et al., 2015) and we also did not see changes in expression with age of genes near aDMPs. Nonetheless, it is likely that the aDMPs mark changes in the (stem) cell that occur on a higher level that do contribute to the ageing process. Age-related changes epigenetic changes show resemblance with the changes seen in cancer and cellular senescence (Teschendorff et al., 2010). For example, the number of passages *in vitro* can be tracked based on the changes that occur on the DNA methylation level (Koch et al., 2012). Moreover, cellular senescence is associated with hypermethylation of CGIs and flanking regions, while hypomethylation occurs on non-CGI features (Cruickshanks et al., 2013; Koch et al., 2013; Schellenberg et al., 2011). Cancer on the other hand is also characterized by hyper methylation of CpG islands and global hypomethylation (Akalin et al., 2012; Irizarry et al., 2009; Schlesinger et al., 2007; Timp and Feinberg, 2013).

A limitation of our study is that our primary set of aDMPs was determined in each tissue in a different group of individuals. To overcome this limitation, we investigated aDMPs also in an independent dataset consisting of 10 tissues of the same individual (N=10-16 per tissue, age range: 44-85 years). Identified differences between tissues were not the result of that we investigated aDMPs in different populations, as the tissue-specificity of the methylation of aDMPs was confirmed in tissues from the same individuals. Another limitation our study is that not all datasets were equally sized. Larger datasets may have more power to find aDMPs. However, as we showed in the results section we did not find a relation between sample size and the number of aDMPs and while the buccal dataset was smallest the number of aDMPs were highest. This suggests that the effect of sample size on the number of aDMPs is limited and this may also be the result of our stringent effect size criteria. Finally, subsets of CpGs have been reported to be the result of changes in cell heterogeneity (Rakyan et al., 2010). Some of the changes identified here may also be the result of a shift in cellular heterogeneity, although we adjusted for cellular heterogeneity in brain (neuronal and non-neuronal), monocytes and Th cells (residual impurities). Furthermore, we did not find indications that loss-aDMPs were the result of changes in cell heterogeneity as the GO terms linked to loss-aDMPs did not show a strong enrichment for cell (subtype) specific processes.

Together, our results show that while in each tissue different CpGs are affected by epigenetic erosion with limited overlap, the functional elements that are affected are the same: gain of methylation at CGIs repressed by PRC2 and loss of methylation at active regions such as enhancers.

METHODS

Datasets

Datasets used in this study are summarized in **Table S1** and were obtained from the Gene Expression Omnibus (Barrett et al., 2013) or ArrayExpress (Kolesnikov et al., 2014). For each of the datasets normalized data or raw IDAT files were obtained.

Generated tissue dataset Samples of 12 tissues from 16 cadavers were taken within 12 hours post-mortem (**Table S1**). Solid tissues were snap frozen for further processing and stored at -80°C. Whole blood from the thoracic cavity was stored in disodium salt dehydrate (EDTA) tubes (BD, United Kingdom). Genomic DNA from blood was isolated using the Qiagen Minikit (Qiagen, Hilden, Germany) according to manufacturer's protocol. Genomic DNA from tissues was isolated using phenol/chlorophorm extraction. Bisulfite-converted DNA was generated using the Zymo EZ DNA Methylation kit (Zymo, Irvine, CA, USA). DNA methylation was measured using the Illumina Infinium HumanMethylation450 BeadChip according to manufacturer's protocol. Initial QC was performed using the R package MethylAid (van Iterson et al., 2014). Raw data underwent quality control using a custom pipeline (for more details see https://git.lumc.nl/molepi/Leiden450K). Briefly, data was normalized using functional normalization (Aryee et al., 2014), and probes were set to missing if ambiguously mapped (Chen et al., 2013), had a high detection p-value (P> 0.01), low bead count (< 3 beads) or low success rate (missing in >95% of the samples). Data is available from GEO under accession number GSE78743.

External tissue datasets IDAT files of DLPFC samples (Age range 0-97 years) were downloaded and underwent the same QC procedure as the generated data (GEO accession number: GSE74193) (Jaffe et al., 2015). Normalized data of buccal (GEO accession number: GSE50759) consisted of 1,202 individuals with an age range of 1-28 years (Berko et al., 2014). Liver data consisted of 147 individuals with age range between 15 and 86, normalized data of 56 individuals (GEO accession number: GSE48325) (Ahrens et al., 2013), normalized data of 32 individuals (GEO accession number: GSE61258) (Horvath et al., 2014), IDAT files (Level 1) of 30 samples from TCGA (TCGA Research Network) and IDAT files of 29 samples were kindly provided by the authors (GSE60753) (Hlady et al., 2014). IDAT files (Level 1) of kidney consisted of 171 individuals with an age range between 15 and 86 and were obtained from TCGA (TCGA Research Network). Normalized data of monocytes (GEO accession number: GSE56046) consisted of 1,202 individuals with an age range of 44-83 years (Reynolds et al., 2014). Normalized data of Th cells (GEO accession number: GSE56047) consisted of 214 individuals with an age range of 45-79 years (Reynolds et al., 2014)). Normalized data of subcutaneous fat (Array Expression accession number: MTAB-1866) consisted of 648 individuals with an age range of 39-85 years (Grundberg et al., 2012). Normalized data of multiple brain regions consisted between 25 and 41 individuals with an age range between 15-114 years (GEO accession number: GSE64509) (Horvath et al., 2015). Raw IDAT files of epidermis and dermis consisted 38 and 40 individuals between 20 and 90 years (GEO accession number: GSE52980) (Vandiver et al., 2015). Normalized data of skeletal muscle consisted of 48 individuals with an age range between 18 and 89 years (GEO accession number: GSE50498) (Zykovich et al., 2014). Raw IDAT

files of thyroid were kindly provided by the authors and consisted of 28 individuals between 23 and 81 years (GEO accession number: GSE53051) (Timp et al., 2014).

External blood datasets DNA methylation blood data consisted of six public datasets of 4,674 individuals (2,650 males and 2,024 females) with an age range 1 to 101 years with median age 50 (**Table S1**). Dataset 1 consisted of 643 whole blood samples and raw IDAT files were kindly provided by the authors and data was normalized as described above (GEO accession number: GSE40279) (Hannum et al., 2013). Dataset 2 consisted of 324 peripheral blood lymphocyte samples and normalized data was downloaded from GEO (GEO accession number: GSE51032). Dataset 3 consisted of 327 peripheral blood lymphocyte samples and raw data was normalized as described above (GEO accession number: GSE42861) (Liu et al., 2013). Dataset 4 consisted of 127 peripheral blood lymphocyte samples and raw data was normalized as described above (GEO accession number: GSE36054) (Alisch et al., 2012). Dataset 5 consisted of 614 peripheral blood lymphocyte samples and normalized data was downloaded from GEO (GEO accession number: GSE56105) (Shah et al., 2014). Dataset 6 consisted of 2639 whole blood samples and normalized data was downloaded from GEO (GEO accession number: GSE55763) (Lehne et al., 2015).

Gene expression Gene counts were obtained from GTEX (Lonsdale et al., 2013) for frontal cortex (for brain-aDMPs measured in DLPFC), esophagus mucosa (for buccal-aDMPs), liver, kidney cortex and whole blood (for Th cell-aDMPs and monocyte-aDMPs). The package cqn was used to normalize for GC content and gene length (Hansen et al., 2012). Normalized data was used to calculate the average RPKM per tissue and gene.

Age-related changes

aDMPs were identified using linear regression between DNA methylation and age, with adjustment for covariates (sex, gender (all but SAT, females only), dataset (liver), cell composition (DLPFC, monocytes, Th cells). aDMPs were used in subsequent analyses if the slope was higher than 2% gain or loss per 10 years and if the Bonferroni adjusted P-value reached significance (P_{bonf} ≤0.05). Age-related changes were also investigated in the independent generated dataset described above. Slopes of identified aDMPs were determined in this dataset by fitting a linear model of methylation versus age adjusted for gender.

Annotations CpGs were mapped to CpG islands (UCSC), shores (2kb regions flanking regions) and non-CGI described previously (Slieker et al., 2013). Chromatin state segmentations were obtained from the Epigenomics Roadmap (Roadmap Epigenomics Consortium et al., 2015). For each tissue studied the same tissue or the closest analogue was used from the Roadmap data. For the DLPFC, E073/DLPFC was used; buccal, E058/keratinocyte foreskin; liver, E066/liver; kidney, E086/fetal kidney; SAT, E063/Adipose nuclei; monocytes, E029/Monocytes; Th cells, E043/Th cells. ChIP-seq data of transcription factor binding sites (such as EZH2) were obtained for all cell types from the ENCODE project (ENCODE, 2012). Enrichments were expressed as odds ratio and P-value was calculated using a chi-squared test. GO enrichment was performed using the default settings of DAVID using nearest genes of aDMPs (Huang et al., 2009).

REFERENCES

Ahrens, M., Ammerpohl, O., von Schönfels, W., Kolarova, J., Bens, S., Itzel, T., Teufel, A., Herrmann, A., Brosch, M., and Hinrichsen, H. (2013). DNA methylation analysis in nonalcoholic fatty liver disease suggests distinct disease-specific and remodeling signatures after bariatric surgery. Cell metabolism 18, 296-302.

Akalin, A., Garrett-Bakelman, F.E., Kormaksson, M., Busuttil, J., Zhang, L., Khrebtukova, I., Milne, T.A., Huang, Y., Biswas, D., and Hess, J.L. (2012). Base-pair resolution DNA methylation sequencing reveals profoundly divergent epigenetic landscapes in acute myeloid leukemia. PLoS Genet 8, e1002781.

Alisch, R.S., Barwick, B.G., Chopra, P., Myrick, L.K., Satten, G.A., Conneely, K.N., and Warren, S.T. (2012). Age-associated DNA methylation in pediatric populations. Genome research 22, 623-632.

Aryee, M.J., Jaffe, A.E., Corrada-Bravo, H., Ladd-Acosta, C., Feinberg, A.P., Hansen, K.D., and Irizarry, R.A. (2014). Minfi: a flexible and comprehensive Bioconductor package for the analysis of Infinium DNA methylation microarrays. Bioinformatics, btu049.

Barrett, T., Wilhite, S.E., Ledoux, P., Evangelista, C., Kim, I.F., Tomashevsky, M., Marshall, K.A., Phillippy, K.H., Sherman, P.M., and Holko, M. (2013). NCBI GEO: archive for functional genomics data sets—update. Nucleic acids research 41, D991-D995.

Bekaert, B., Kamalandua, A., Zapico, S.C., Van de Voorde, W., and Decorte, R. (2015). Improved age determination of blood and teeth samples using a selected set of DNA methylation markers. Epigenetics 10, 922-930.

Bell, J.T., Tsai, P.-C., Yang, T.-P., Pidsley, R., Nisbet, J., Glass, D., Mangino, M., Zhai, G., Zhang, F., and Valdes, A. (2012). Epigenome-wide scans identify differentially methylated regions for age and age-related phenotypes in a healthy ageing population. PLoS Genet 8, e1002629.

Berko, E.R., Suzuki, M., Beren, F., Lemetre, C., Alaimo, C.M., Calder, R.B., Ballaban-Gil, K., Gounder, B., Kampf, K., and Kirschen, J. (2014). Mosaic epigenetic dysregulation of ectodermal cells in autism spectrum disorder. PLoS genetics 10.

Chen, Y.-a., Lemire, M., Choufani, S., Butcher, D.T., Grafodatskaya, D., Zanke, B.W., Gallinger, S., Hudson, T.J., and Weksberg, R. (2013). Discovery of cross-reactive probes and polymorphic CpGs in the Illumina Infinium HumanMethylation450 microarray. Epigenetics 8, 203-209.

Cruickshanks, H.A., McBryan, T., Nelson, D.M., VanderKraats, N.D., Shah, P.P., van Tuyn, J., Rai, T.S., Brock, C., Donahue, G., and Dunican, D.S. (2013). Senescent cells harbour features of the cancer epigenome. Nature cell biology 15, 1495-1506.

Day, K., Waite, L.L., Thalacker-Mercer, A., West, A., Bamman, M.M., Brooks, J.D., Myers, R.M., and Absher, D. (2013). Differential DNA methylation with age displays both common and dynamic features across human tissues that are influenced by CpG landscape. Genome Biol 14, R102.

Dozmorov, M.G. (2015). Polycomb Repressive Complex 2 epigenomic signature defines age-associated hypermethylation and gene expression changes. Epigenetics, 1-12.

ENCODE (2012). An integrated encyclopedia of DNA elements in the human genome. Nature 489, 57-74.

Fernández, A.F., Bayón, G.F., Urdinguio, R.G., Toraño, E.G., García, M.G., Carella, A., Petrus-Reurer, S., Ferrero, C., Martinez-Camblor, P., and Cubillo, I. (2014). H3K4me1 marks DNA regions hypomethylated during aging in stem and differentiated cells. Genome research.

Florath, I., Butterbach, K., Müller, H., Bewerunge-Hudler, M., and Brenner, H. (2014). Cross-sectional and longitudinal changes in DNA methylation with age: an epigenome-wide analysis revealing over 60 novel age-associated CpG sites. Human molecular genetics 23, 1186-1201.

Garagnani, P., Bacalini, M.G., Pirazzini, C., Gori, D., Giuliani, C., Mari, D., Di Blasio, A.M., Gentilini, D., Vitale, G., and Collino, S. (2012). Methylation of *ELOVL2* gene as a new epigenetic marker of age. Aging cell 11, 1132-1134.

Grundberg, E., Small, K.S., Hedman, Å.K., Nica, A.C., Buil, A., Keildson, S., Bell, J.T., Yang, T.-P., Meduri, E., and Barrett, A. (2012). Mapping cis- and trans-regulatory effects across multiple tissues in twins. Nature genetics 44, 1084-1089.

Hannum, G., Guinney, J., Zhao, L., Zhang, L., Hughes, G., Sadda, S., Klotzle, B., Bibikova, M., Fan, J.B., Gao, Y., et al. (2013). Genome-wide methylation profiles reveal quantitative views of human aging rates. Molecular cell 49, 359-367.

Hansen, K.D., Irizarry, R.A., and Zhijin, W. (2012). Removing technical variability in RNA-seq data using conditional quantile normalization. Biostatistics 13, 204-216.

Hernandez, D.G., Nalls, M.A., Gibbs, J.R., Arepalli, S., van der Brug, M., Chong, S., Moore, M., Longo, D.L., Cookson, M.R., and Traynor, B.J. (2011). Distinct DNA methylation changes highly correlated with chronological age in the human brain. Human molecular genetics 20, 1164-1172.

Hlady, R.A., Tiedemann, R.L., Puszyk, W., Zendejas, I., Roberts, L.R., Choi, J.-H., Liu, C.,

and Robertson, K.D. (2014). Epigenetic signatures of alcohol abuse and hepatitis infection during human hepatocarcinogenesis. Oncotarget 5, 9425.

Horvath, S. (2013). DNA methylation age of human tissues and cell types. Genome biology 14, R115.

Horvath, S., Erhart, W., Brosch, M., Ammerpohl, O., von Schönfels, W., Ahrens, M., Heits, N., Bell, J.T., Tsai, P.-C., and Spector, T.D. (2014). Obesity accelerates epigenetic aging of human liver. Proceedings of the National Academy of Sciences 111, 15538-15543.

Horvath, S., Mah, V., Lu, A.T., Woo, J.S., Choi, O.-W., Jasinska, A.J., Riancho, J.A., Tung, S., Coles, N.S., and Braun, J. (2015). The cerebellum ages slowly according to the epigenetic clock. Aging 7.

Huang, D.W., Sherman, B.T., and Lempicki, R.A. (2009). Systematic and integrative analysis of large gene lists using DAVID bioinformatics resources. Nature protocols 4, 44-57.

Irizarry, R.A., Ladd-Acosta, C., Wen, B., Wu, Z., Montano, C., Onyango, P., Cui, H., Gabo, K., Rongione, M., and Webster, M. (2009). The human colon cancer methylome shows similar hypo-and hypermethylation at conserved tissue-specific CpG island shores. Nature genetics 41, 178-186.

Ismail, I.H., Gagné, J.-P., Caron, M.-C., McDonald, D., Xu, Z., Masson, J.-Y., Poirier, G.G., and Hendzel, M.J. (2012). CBX4-mediated SUMO modification regulates BMI1 recruitment at sites of DNA damage. Nucleic acids research 40, 5497-5510.

Jaffe, A.E., Gao, Y., Deep-Soboslay, A., Tao, R., Hyde, T.M., Weinberger, D.R., and Kleinman, J.E. (2015). Mapping DNA methylation across development, genotype and schizophrenia in the human frontal cortex. Nat Neurosci advance online publication.

Johansson, Å., Enroth, S., and Gyllensten, U. (2013). Continuous aging of the human DNA methylome throughout the human lifespan. PLoS One 8, e67378.

Jung, M., and Pfeifer, G.P. (2015). Aging and DNA methylation. BMC biology 13, 7.

Koch, C.M., Joussen, S., Schellenberg, A., Lin, Q., Zenke, M., and Wagner, W. (2012). Monitoring of cellular senescence by DNA-methylation at specific CpG sites. Aging cell 11, 366-369.

Koch, C.M., Reck, K., Shao, K., Lin, Q., Joussen, S., Ziegler, P., Walenda, G., Drescher, W., Opalka, B., and May, T. (2013). Pluripotent stem cells escape from senescence-associated DNA methylation changes. Genome research 23, 248-259.

Kolesnikov, N., Hastings, E., Keays, M., Melnichuk, O., Tang, Y.A., Williams, E., Dylag, M., Kurbatova, N., Brandizi, M., and Burdett, T. (2014). ArrayExpress update—Simplifying data submissions. Nucleic acids research, gku1057.

Lehne, B., Drong, A.W., Loh, M., Zhang, W., Scott, W.R., Tan, S.-T., Afzal, U., Scott, J., Jarvelin, M.-R., and Elliott, P. (2015). A coherent approach for analysis of the Illumina HumanMethylation450 BeadChip improves data quality and performance in epigenome-wide association studies. Genome biology 16, 37.

Liu, Y., Aryee, M.J., Padyukov, L., Fallin, M.D., Hesselberg, E., Runarsson, A., Reinius, L., Acevedo, N., Taub, M., and Ronninger, M. (2013). Epigenome-wide association data implicate DNA methylation as an intermediary of genetic risk in rheumatoid arthritis. Nature biotechnology 31, 142-147.

Lonsdale, J., Thomas, J., Salvatore, M., Phillips, R., Lo, E., Shad, S., Hasz, R., Walters, G., Garcia, F., and Young, N. (2013). The genotype-tissue expression (GTEx) project. Nature genetics 45, 580-585.

Maegawa, S., Hinkal, G., Kim, H.S., Shen, L., Zhang, L., Zhang, J., Zhang, N., Liang, S., Donehower, L.A., and Issa, J.-P.J. (2010). Widespread and tissue specific age-related DNA methylation changes in mice. Genome research 20, 332-340.

Marttila, S., Kananen, L., Häyrynen, S., Jylhävä, J., Nevalainen, T., Hervonen, A., Jylhä, M., Nykter, M., and Hurme, M. (2015). Ageing-associated changes in the human DNA methylome: genomic locations and effects on gene expression. BMC genomics 16, 179.

McClay, J.L., Aberg, K.A., Clark, S.L., Nerella, S., Kumar, G., Xie, L.Y., Hudson, A.D., Harada, A., Hultman, C.M., and Magnusson, P.K. (2014). A methylome-wide study of aging using massively parallel sequencing of the methyl-CpG-enriched genomic fraction from blood in over 700 subjects. Human molecular genetics 23, 1175-1185.

Peters, M.J., Joehanes, R., Pilling, L.C., Schurmann, C., Conneely, K.N., Powell, J., Reinmaa, E., Sutphin, G.L., Zhernakova, A., and Schramm, K. (2015). The transcriptional landscape of age in human peripheral blood. Nature communications 6.

Polesskaya, A., Cuvellier, S., Naguibneva, I., Duquet, A., Moss, E.G., and Harel-Bellan, A. (2007). Lin-28 binds IGF-2 mRNA and participates in skeletal myogenesis by increasing translation efficiency. Genes & development 21, 1125-1138.

Rakyan, V.K., Down, T.A., Maslau, S., Andrew, T., Yang, T.-P., Beyan, H., Whittaker, P., McCann, O.T., Finer, S., and Valdes, A.M. (2010). Human aging-associated DNA hypermethylation occurs preferentially at bivalent chromatin domains. Genome research 20, 434-439.

Reynolds, L.M., Taylor, J.R., Ding, J., Lohman, K., Johnson, C., Siscovick, D., Burke, G.,

Post, W., Shea, S., Jacobs Jr, D.R., et al. (2014). Age-related variations in the methylome associated with gene expression in human monocytes and T cells. Nat Commun 5.

Richardson, R.B., Allan, D.S., and Le, Y. (2014). Greater organ involution in highly proliferative tissues associated with the early onset and acceleration of ageing in humans. Experimental gerontology 55, 80-91.

Roadmap Epigenomics Consortium, Kundaje, A., Meuleman, W., Ernst, J., Bilenky, M., Yen, A., Heravi-Moussavi, A., Kheradpour, P., Zhang, Z., Wang, J., et al. (2015). Integrative analysis of 111 reference human epigenomes. Nature 518, 317-330.

Rönn, T., Volkov, P., Gillberg, L., Kokosar, M., Perfilyev, A., Jacobsen, A.L., Jørgensen, S.W., Brøns, C., Jansson, P.-A., and Eriksson, K.-F. (2015). Impact of age, BMI and HbA1c levels on the genome-wide DNA methylation and mRNA expression patterns in human adipose tissue and identification of epigenetic biomarkers in blood. Human molecular genetics 24, 3792-3813.

Schellenberg, A., Lin, Q., Schüler, H., Koch, C.M., Joussen, S., Denecke, B., Walenda, G., Pallua, N., Suschek, C.V., and Zenke, M. (2011). Replicative senescence of mesenchymal stem cells causes DNA-methylation changes which correlate with repressive histone marks. Aging (Albany NY) 3, 873.

Schlesinger, Y., Straussman, R., Keshet, I., Farkash, S., Hecht, M., Zimmerman, J., Eden, E., Yakhini, Z., Ben-Shushan, E., and Reubinoff, B.E. (2007). Polycomb-mediated methylation on Lys27 of histone H3 pre-marks genes for de novo methylation in cancer. Nature genetics 39, 232-236.

Shah, S., McRae, A.F., Marioni, R.E., Harris, S.E., Gibson, J., Henders, A.K., Redmond, P., Cox, S.R., Pattie, A., and Corley, J. (2014). Genetic and environmental exposures constrain epigenetic drift over the human life course. Genome research 24, 1725-1733.

Slieker, R.C., Bos, S.D., Goeman, J.J., Bovée, J., Talens, R.P., van der Breggen, R., Suchiman, H., Lameijer, E.-W., Putter, H., and van den Akker, E.B. (2013). Identification and systematic annotation of tissue-specific differentially methylated regions using the Illumina 450k array. Epigenetics Chromatin 6, 26.

Spiers, H., Hannon, E., Wells, S., Williams, B., Fernandes, C., and Mill, J. (2016). Age-associated changes in DNA methylation across multiple tissues in an inbred mouse model. Mech Ageing Dev 154:20-3.

Steegenga, W.T., Boekschoten, M.V., Lute, C., Hooiveld, G.J., de Groot, P.J., Morris, T.J., Teschendorff, A.E., Butcher, L.M., Beck, S., and Müller, M. (2014). Genome-wide age-related changes in DNA methylation and gene expression in human PBMCs. Age 36, 1523-1540.

TCGA Research Network. http://cancergenome.nih.gov/.

Teschendorff, A.E., Menon, U., Gentry-Maharaj, A., Ramus, S.J., Weisenberger, D.J., Shen, H., Campan, M., Noushmehr, H., Bell, C.G., and Maxwell, A.P. (2010). Age-dependent DNA methylation of genes that are suppressed in stem cells is a hallmark of cancer. Genome research 20, 440-446.

Timp, W., Bravo, H.C., McDonald, O.G., Goggins, M., Umbricht, C., Zeiger, M., Feinberg, A.P., and Irizarry, R.A. (2014). Large hypomethylated blocks as a universal defining epigenetic alteration in human solid tumors. Genome Med 6, 61.

Timp, W., and Feinberg, A.P. (2013). Cancer as a dysregulated epigenome allowing cellular growth advantage at the expense of the host. Nature Reviews Cancer 13, 497-510.

Tomasetti, C., and Vogelstein, B. (2015). Variation in cancer risk among tissues can be explained by the number of stem cell divisions. Science 347, 78-81.

van Iterson, M., Tobi, E., Slieker, R., den Hollander, W., Luijk, R., Slagboom, P., and Heijmans, B. (2014). MethylAid: Visual and interactive quality control of large Illumina 450k data sets. Bioinformatics 30(23):3435-7.

Vandiver, A.R., Irizarry, R.A., Hansen, K.D., Garza, L.A., Runarsson, A., Li, X., Chien, A.L., Wang, T.S., Leung, S.G., and Kang, S. (2015). Age and sun exposure-related widespread genomic blocks of hypomethylation in nonmalignant skin. Genome biology 16, 80.

Weidner, C.I., Lin, Q., Koch, C.M., Eisele, L., Beier, F., Ziegler, P., Bauerschlag, D.O., Jöckel, K.-H., Erbel, R., and Mühleisen, T.W. (2014). Aging of blood can be tracked by DNA methylation changes at just three CpG sites. Genome biology 15, R24.

Xu, Z., and Taylor, J.A. (2014). Genome-wide age-related DNA methylation changes in blood and other tissues relate to histone modification, expression and cancer. Carcinogenesis 35, 356-364.

Yuan, T., Jiao, Y., de Jong, S., Ophoff, R.A., Beck, S., and Teschendorff, A.E. (2015). An integrative multi-scale analysis of the dynamic DNA methylation landscape in aging. PLoS genetics 11, e1004996-e1004996.

Zykovich, A., Hubbard, A., Flynn, J.M., Tarnopolsky, M., Fraga, M.F., Kerksick, C., Ogborn, D., MacNeil, L., Mooney, S.D., and Melov, S. (2014). Genome-wide DNA methylation changes with age in disease-free human skeletal muscle. Aging Cell 13, 360-366.